

Calculation Methods for Digital Model Creation Based on Integrated Shape, Color and Angular Reflectivity Measurement

Robert Sitnik, Grzegorz Mączkowski, and Jakub Krzesłowski

WUT, Institute of Micromechanics and Photonics, 8 Boboli, 02-525 Warsaw, Poland
{r.sitnik,g.maczkowski,j.krzeslowski}@mchtr.pw.edu.pl

Abstract. The paper presents a complete methodology for processing sets of data registered by the means of a measurement system providing integrated 3D shape, multispectral color and angular reflectance characteristic. The data comprise of clouds of points representing the shape of the measured object, a set of intensity responses as a function of wavelength of incident light used for color calculation and a set of distributions of reflected intensity as a function of illumination and observation angles. Presented approach allows to create a complete 3D model of the measured object which preserves the object's shape, color and reflectivity properties. It is developed specifically for application in the digitization of cultural heritage objects for storing and visualization purposes, as well as duplication by the means of 3D printing technology.

Keywords: cultural heritage digitization, structured light projection, multispectral color, BRDF, cloud of points, triangle mesh, texture, calculation methods.

1 Integrated System for Cultural Heritage Objects Digitization

1.1 Introduction

Recently, different techniques for digitization of many classes of objects have emerged. They usually require specific data processing methods and vary greatly because of different technologies involved, different accuracy and applications. A review of different approaches to shape digitization depending on object's size, material and complexity was given by Pavlidis et al. [1]. There also exist several studies involving multispectral color measurements of oil paintings [2]. Different implementations of such devices vary in the number of registered spectral bands and data processing algorithms depending on specific application [3], [4]. Consequently, there are different possibilities of registering angular reflectance, either by time consuming gonio-reflectometry or a kind of simplified bidirectional reflectance distribution function (BRDF) estimation similar to extended photometric stereo [5]. Nevertheless, combining these kinds of data together to create a more precise representation of the object usually requires some manual processing to fit the data from different measurement devices into a single, complete model.

In this paper we would like to focus on digital measurements of cultural heritage objects based on the measurement of integrated shape, multispectral color and angular reflectance characteristic [6]. In this case, directional illumination is used for BRDF estimation, but with additional knowledge of surface position and its normal vectors. The main purpose of this research is the registration of object's appearance with good accuracy for storing in a digital archive, visualization and duplication. We propose a set of calculation methods which allow to obtain a complete virtual model from raw data acquired with the 3D scanner.

At the beginning of the paper the measurement system is presented along with the data format used in calculation methods. It is followed by the description of the concept of data processing methodology and its implementation, after which detailed descriptions of implemented algorithms are provided along with exemplary results of their application in experimental measurements.

1.2 Measurement System Description

The system incorporates a 3D scanner, a multispectral camera for color measurement and a custom designed angular reflectance measurement device. The fact that all the components use the same detector eliminates the need for manual alignment of the acquired data, as all the necessary information is provided for every point registered on the measured surface unambiguously.

The shape measurement system comprises of a digital light projector and a CCD camera which are calibrated together. Its operation relies on structured light projection [7] and it allows for registering shape of the investigated surface within a 200 x 300 x 200mm measurement volume with 0.1mm resolution and 0.03mm accuracy (Fig. 1).

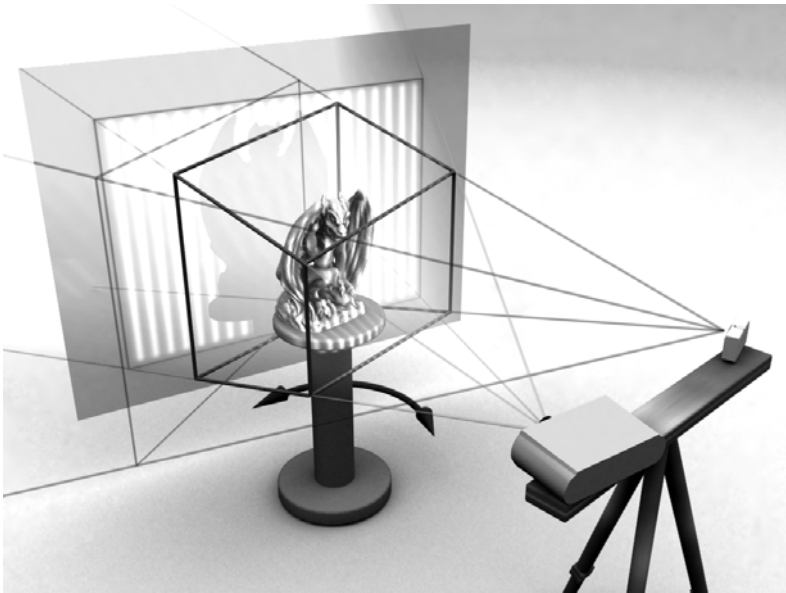


Fig. 1. 3D shape measurement system

The color measurement system [6] uses a multispectral approach based on capturing images of the object in several different spectral bands under specified, known illumination. The system measures spectral reflectance distribution in every point registered by the camera. In the described setup a custom built multispectral camera with 20 spectral bands and flash as a light source was used (Fig. 2)

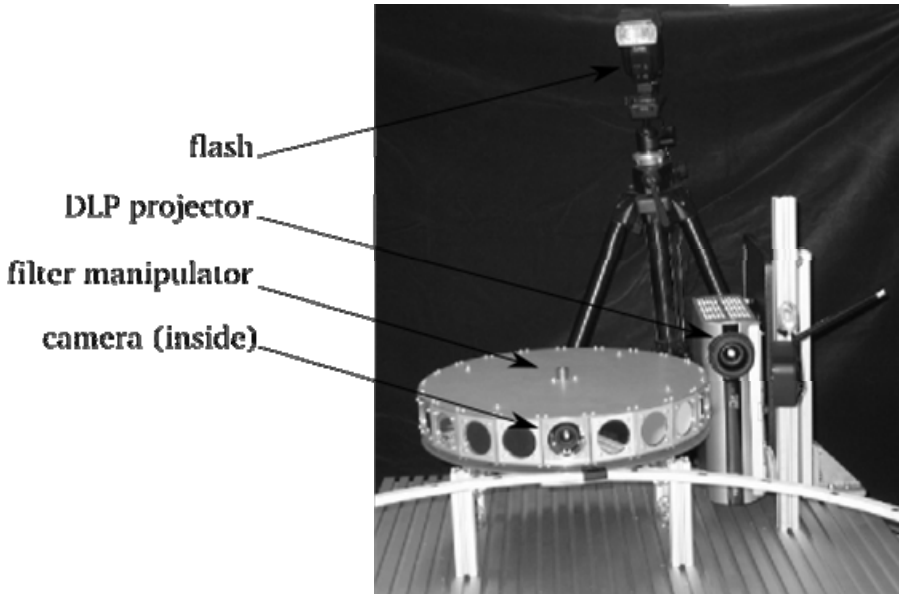


Fig. 2. Multispectral camera integrated with the 3D shape measurement system

For angular reflection measurement [6] a specially designed setup was used, which supports controlled directional illumination of the investigated surface from several known positions relative to the direction of observation. Eleven uniformly distributed white light emitting diodes with additional diffusers were used as light sources.

1.3 Raw Data from the Measurement

Data registered in the integrated measurement include space coordinates of the surface. Additionally, a set of reflected energy responses in several spectral bands within the visible spectrum and a set of luminous energy responses from several angles of illumination are independently acquired for every point. Other data resulting from the measurement include spectral emission characteristic of a light source, optical setup attenuation and geometry of angular light sources distribution.

The data are organized in a structure in order to simplify further processing. The basic structure is a cloud of points with normal vectors calculated in every point based on its local neighbourhood. The rest of the data is assigned to the cloud of points as additional layers in such a way, that each point in the cloud can have a vector of properties attached. In the case of integrated measurement, the previously described information containing energy responses from spectral and angular measurements is stored in this

vector. The whole structure can be extended to make it possible to add other data layers and increase the dimension of the attached vector of properties. The data structure is stored in several binary files with a single XML interface, which makes it easy to manage and extend. The scheme of the data structure is shown in Fig. 3.

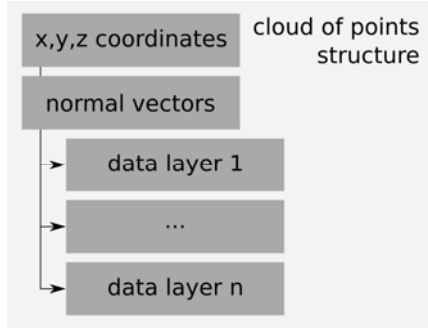


Fig. 3. Diagram of a basic data structure for storing cloud of points geometrical data with additional point information

2. Data Processing Path

2.1 The Concept

Data registered in a single measurement process can be divided into three separate categories, as mentioned in the previous section. The first category is shape in the form of cloud of points, the second is spectral reflectance and the third – angular reflectance (Fig. 4).

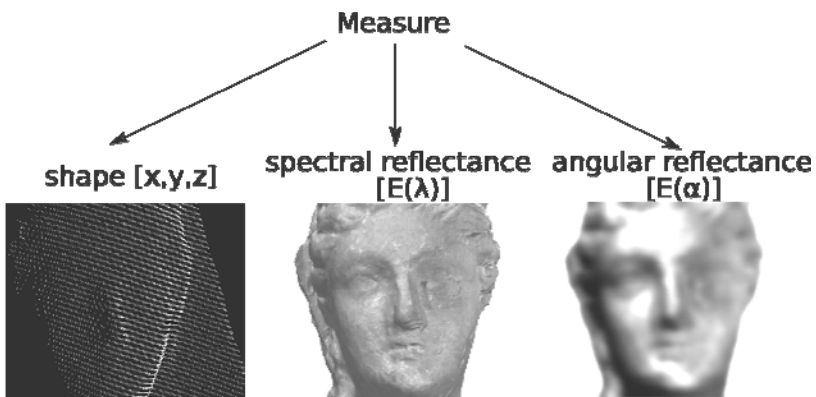


Fig. 4. Categories of surface measurement data, which can be processed by various calculation methods and combined into a 3D model

We propose three final stages for the processed data depending on their application – storing in a digital archive, displaying in a virtual scene and duplication by the means of 3D printing technology. It is therefore necessary to propose different processing paths for each implementation. In order to use intermediate processing stages efficiently, applied operations are designed in a way which allows them to make use of results from previous processing stages. A flowchart in Fig. 5 shows relations between the processing stages.

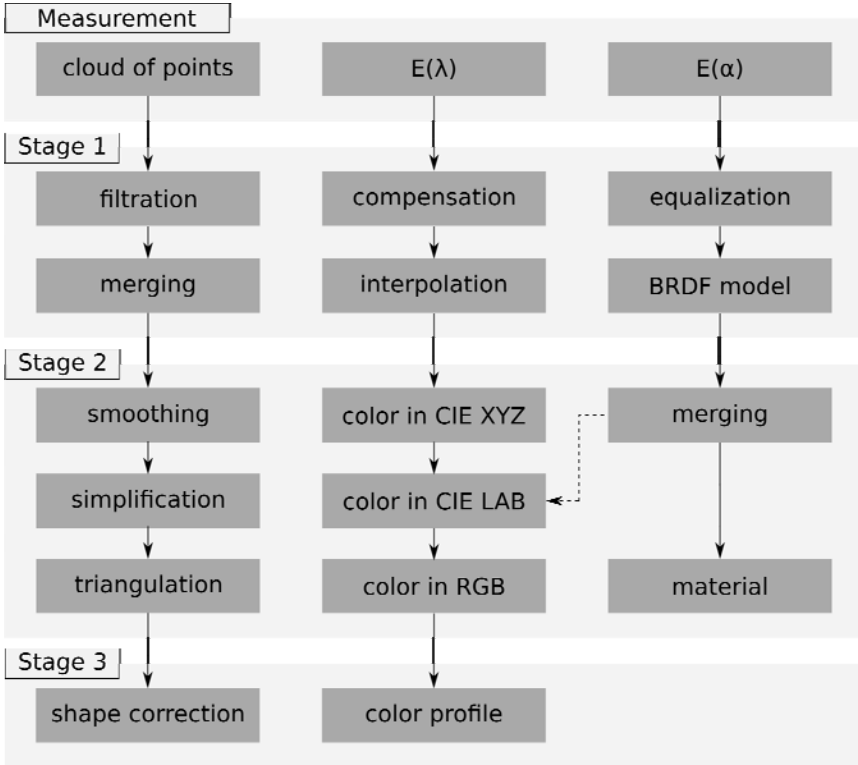


Fig. 5. Diagram of three data processing stages and three main processing paths (one for each data category). It should be noted that even though the processing paths are not joint, some calculation methods use a portion of output from the other paths.

In the first stage, data are processed for storing in a digital archive. Clouds of points are filtered in order to eliminate noise and errors caused by incorrect phase calculation. Next, the clouds acquired from several different directions are merged with the use of ICP algorithms [8] in order to create a full model of the measured object. At this stage the shape data are considered sufficient for storage purposes.

Color measurement data are interpolated over the visible spectrum domain, so that spectral reflectance for each point in the cloud of points can be estimated. Other calibration data, including emission spectrum characteristic of the light source used in the

measurement, correction coefficients of the field's of view uniformity and spectral filters' energy compensation factors are necessary for this operation.

Angular reflectance measurement data are used for a BRDF derivation according to Phong model [9]. Additional calibration data used include black component compensation factors and information about the distribution of light sources in space.

The second stage of operations is used for obtaining a model adequate for display in a virtual environment. It is based on the data received from the previous stage rather than on the raw measurement data.

At this moment the complete 3D model represented as a set of dense clouds of points constitute the input shape measurement data. First it is smoothed to eliminate noise and improve the quality of clouds' fit. Next the clouds are simplified in order to decrease the amount of superfluous data while preserving the curvature of model's surfaces. Finally comes the triangulation procedure which produces a triangle mesh, which then needs to be filtered and smoothed.

Color data processing for visualisation relies on the calculation of color coordinates from estimated spectral reflectance. First the colors are represented in the CIE XYZ color space for a chosen standard illuminant, and then transformed into the CIE $L^*a^*b^*$ color space, where the L^* coordinate can be exchanged for the intensity value calculated from Phong parameters based on the angular reflectance measurement. This allows to include material properties directly in the texture of objects with lambertian angular reflectance characteristic. Afterwards color profile in RGB color space necessary for the displaying device color is calculated. This data, along with mapping coordinates assigned to the triangle mesh, create the texture for the model. The Phong parameters, modelling the BRDF of the surface can be used to determine material properties for realistic rendering with the use of arbitrary illumination conditions of the virtual scene.

Consequently, the result of the second stage of data processing is a model represented as a triangle mesh with mapped texture along with material reflectivity characteristic. It can be exported to VRML format for use in a variety of renderings software to create static or animated renderings for online, as well as offline visualisation.

The purpose of the third stage of processing is the preparation of data for a color 3D printer in order to produce copies of digitized objects. As before, the data from previous stage (in this case the triangle mesh and $L^*a^*b^*$ color coordinates) are used as input.

As for the printing technology, 3DP is assumed, which requires application of a procedure for compensating shape deviation of the model due to shrinkage of material during the printing process. Therefore an analytical model is applied to the triangle mesh which enhances its shape in order to get more precise correspondence between the original object and its copy.

Additionally a color profile for the 3D printer based on local interpolation of a set of representative reference color samples is applied. This allows to take into account limited color resolution of the color 3D printer.

2.2 Integration with 3DMADMAC Environment

All mentioned operations are implemented as separate calculation methods which work within the 3DMADMAC environment [10]. The calculation methods can be

exchanged easily, as well as combined into more complicated calculation patterns, as they work as independent plug-ins supplied in DLL libraries. This allows the user to customize the processing path to meet the needs of a specific application and even extend the functionality of the system by adding new calculation methods.

3 Implementation

3.1 3D Shape Calculation Methods

Clouds of Points Filtering. Usually a cloud of points registered in a shape measurement has uniform density distribution of points in the middle of the measurement volume, whereas on borders and in parts with sharp edges points are more sparse and more prone to noise. Such points need to be filtered out and replaced by data acquired from other directions. The filtration procedure [11] relies on finding small groups of points separated from each other farther than the average distance between points in the cloud multiplied by a predefined constant, which are then deleted from the cloud.

Merging Clouds of Points. The procedure of fitting directional clouds of points [12] can be divided into two steps. First, a coarse fitting algorithm is applied, which calculates an additional data layer with curvature coefficients of a surface. After that segmentation is performed on the curvature data layer and similar segments from adjacent clouds of points are merged together. The second step of clouds' fitting incorporates the ICP algorithm [8], which minimizes the root mean square error between corresponding points in roughly fitted clouds by applying small orientation and translation adjustments to the position of one of the clouds.

Smoothing Clouds of Points. In order to minimize the noise resulting from phase calculation as well as small imprecision of fitting the clouds a smoothing algorithm [11] is applied, which fits a plane to a small neighbourhood of every point and changes its position based on the neighbourhood if the distance to such plane is bigger than a specified threshold.

Simplification of Clouds of Points. In most cases clouds of points taken directly from a measurement are too dense to be the source of a triangle mesh, because the procedure would create unreasonably many triangles, which would be very difficult to manage with restricted software resources. Clouds of points therefore usually require simplification – which can be either a uniform process or done using an adaptive algorithm which varies the number of points left according to local curvature [13]. When the surface's shape is more complicated i.e. has higher curvature, more points are left for more precise triangle mesh construction. The parameter which constrains the simplification procedure describes maximum deviation of mesh compared to the simplified surface.

Triangulation. Visualisation of a 3D model in an arbitrary virtual scene requires representing the object as a mesh of triangles which can be textured and rendered. Among many triangulation algorithms the one chosen for this stage of processing is

the algorithm developed specifically for creating meshes from clouds of points generated in 3D shape measurements [14]. It generates the mesh in several steps including sharp edges detection, edges triangulation, creation of seed triangles and triangulation of the remaining area. It has very good performance in triangulation of noisy and irregular clouds of points thanks to its optimization in the direction of processing this kind of data.

3.2 Color Calculation Methods

Before interpolation of the spectral reflectance data over the domain covering the visible range of wavelengths, a compensation of the optical setup characteristic is necessary. The proposed system does not distinguish emission spectrum characteristic from detector's sensitivity characteristic, but it is able to compensate them together through calibration using a photographic white reference plate. The reference plate scatters all wavelengths within the visible spectrum uniformly, so its spectral reflectance can be assumed constant. It is possible to prove this through a measurement with a spectrophotometer. Knowing intensity responses from the white reference plate as a function of wavelength, it is possible to perform the compensation. Additionally, transmission characteristics of the spectral filters used for spectrum sampling are energetically normalized according to formula (1) and (2):

$$I(x, y, z) = \frac{I_d(x, y, z)}{t}, \quad (1)$$

$$t = \frac{\int_{\lambda_i - \frac{\Delta\lambda}{2}}^{\lambda_i + \frac{\Delta\lambda}{2}} T(\lambda) d\lambda}{\Delta\lambda \cdot 100\%}. \quad (2)$$

Where $I_d(x, y, z)$ is the intensity registered by the detector for a specific point and $T(\lambda)$ is the transmission characteristic of a spectral filter as a function of wavelength.

Finally input data for interpolation can be described by the formula (3):

$$I_s(r, \lambda) = I(r, \lambda) \frac{C}{I_{\max}} \frac{1}{I_i(r, \lambda) I_a(r, \lambda) T(\lambda)}, \quad (3)$$

where r denotes point's x, y, z coordinates in space, C is a constant corresponding to the intensity level of white reference plate; I_i is the illumination intensity and I_a is the attenuation characteristic of the optical setup. Both I_i and I_a are specified using the calibration data.

Having I_s calculated, an interpolation algorithm is introduced. It interpolates data with $\Delta\lambda$ increments of 5nm and relies on fitting a cubic spline to the sparsely sampled data [15]. This approach is justified by the assumption that the spectral reflectance characteristic of common surfaces is smooth and has a continuous first derivative within its domain.

Color Spaces Calculation. After calculating the spectral reflectance characteristic, it is possible to derive the color in the CIE XYZ color space, assuming spectral characteristic of specific standard illuminant and color matching functions for chosen standard observer. These procedures are widely known and can be found in [16].

Additionally, color values in the CIE $L^*a^*b^*$ color space are possible to derive [17], which allows to apply a procedure for equalization of intensity on clouds of points registered from different directions. One approach takes advantage of normal vectors orientation on a surface and normalizes L^* coordinate for each point in the cloud. The normalization procedure considers neighbourhood of the investigated point which includes points from all clouds overlapping in this neighbourhood. It calculates L^* as a weighted average of its values L_i from different points from the neighbourhood, where the weight factor is a dot product between normal vector \vec{n} in the chosen point and the observation direction \vec{o} , which is constant and parallel to the detector's optical axis (equation 4).

$$L_{norm}(x, y, z) = \frac{\sum_{i=1}^N L_i(x, y, z) \cos(\angle \vec{n}, \vec{o})}{\sum_{i=1}^N \cos(\angle \vec{n}, \vec{o})} \quad (4)$$

This solution favours parts of the surface which are oriented perpendicularly to the observation direction and therefore have higher signal to noise ratio. Apart from this, the influence of specular reflection component on color calculation is diminished. It is also possible to derive an alternative L^* coordinate values from Phong BRDF parameters estimated from angular reflection measurement.

Having calculated the color in CIE XYZ or $L^*a^*b^*$ coordinates allows for further processing in order to apply a color profile for a specific display device, such as an LCD monitor or a 3D printer, to reproduce colors faithfully. These operations can be implemented as separate calculation methods.

The color profile for a color 3D printer is based on a series of 729 predefined samples' color values spaced uniformly within the printer's dynamic range, which had

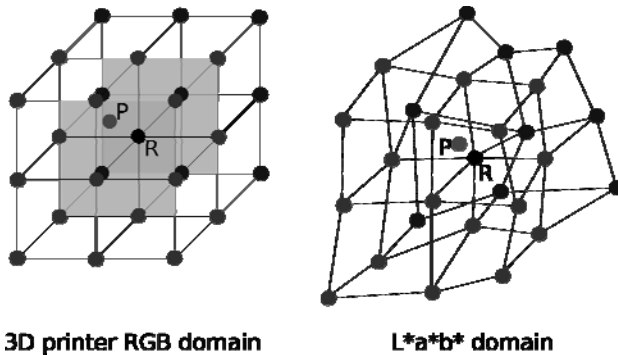


Fig. 6. Local interpolation of color values for a 3D printer color profile

been measured by a reference spectrophotometer to determine their $L^*a^*b^*$ values. The profile should enable to transform from arbitrary $L^*a^*b^*$ color values into printer specific RGB coordinates. To achieve this a local interpolation algorithm is proposed (Fig. 6). For each specific input $L^*a^*b^*$ color coordinates (point P), it searches for the nearest neighbour R within the reference color samples and it calculates the printer RGB values as a weighted average of RGB values from direct neighbours of the R color point with distances between the point P and these neighbours in the $L^*a^*b^*$ domain as the weights.

3.3 Angular Reflectance Calculation Methods

To estimate the intrinsic angular reflectance [18] properties of the investigated surface, several steps are taken before creating a parameterized BRDF representation.

By the use of a reference plate mentioned above, the illuminating setup is calibrated for inequalities of light source intensities for a given geometrical model of their spatial distribution. Based on the geometrical relation between reference lambertian surface, the camera and every light source, compensation coefficients are derived and saved within the calibration framework.

From every directional illumination frame, a dark frame is subtracted for eliminating background bias. After the intensity of directional illumination frames is compensated, for every point a set of halfway versors is derived. The halfway versor \vec{h} lies on the angle bisector between the reflection and viewing directional vectors (\vec{r} and \vec{v} , respectively), and is calculated according to equations (5) and (6).

$$\vec{r} = m(\vec{i}, \vec{n}), \quad (5)$$

$$\vec{h} = \frac{\vec{r} + \vec{v}}{|\vec{r} + \vec{v}|} \quad (6)$$

To calculate the ratio between luminance and illuminance, the photometric law is applied. The incident intensity is multiplied by the inverse product of square distance from the light source and the cosine of incident angle. Both x , y , z coordinates and normal vector are taken from the previously calculated cloud of points structure. The halfway angles [19] are calculated as the dot product of every halfway versor in array and the unit length normal vector at the analysed point. Then the array of reflectance ratios ordered by ascending halfway angle, referred to as the response array, is used for BRDF model fitting (Fig. 7).

BRDF Estimation. Two methods were implemented for retrieving Phong components based on such prepared measurement data. First method incorporates the use of a nonlinear solver, where diffuse, specular and shininess terms are controlled by the RMS value of the overall BRDF slice fitted to data samples. This method produces best results, but it is time consuming and inappropriate for processing the whole cloud of points.

The second method was designed for speed of calculation and takes consecutive steps in order to calculate the three components. Starting from estimation of the diffusive component, the last term of response array is assumed to have the least contribution

from specular reflection. This value is then subtracted from all the other higher values. Then, the specular coefficient is taken from the highest value in the array. The shininess is estimated based on the highest slope of remaining values.

This method is fast but introduces several limitations. For ill positioned points of measured surface, the halfway angle is never equal zero, and so the specular parameter is lower than expected. For this purpose a method of further data processing is introduced, based on the premise, that data merged from several directions introduce different error of angular reflection estimation.

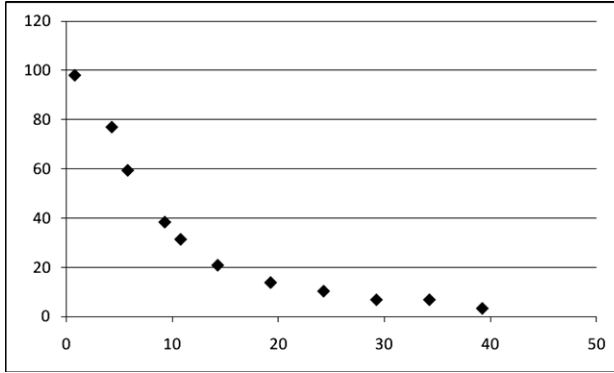


Fig. 7. Depiction of a response array of ordered reflectance values in a descending fashion

Reflectance Quality Factors. Apart from three data layers of Phong parameters created by the means of single directional measurement calculation, an additional data layer of quality factors is saved for every directional cloud of points. These quality factors are inverse values of the lowest halfway angle calculated in the previous methods. The data layer of quality factors correlates to the systematic error of specular reflection estimation at every point of the surface geometrical model.

BRDF Data Merging. For clouds of points measured from different directions and fitted using the ICP algorithm, the quality factors of locally corresponding points may have higher values and manifest better estimation of specular and shininess components. By the means of local averaging of these components, quality factors are used as weights. This way for every point P_i and a set of neighbouring points P_i within radius r coming from different directional measurements, specular k_s and shininess k_e components are corrected in the following relation (equation 7):

$$k_{s,e}(P_1)^{(new)} = \frac{k_{s,e}(P_1)^{(old)} \cdot q(P_1) + \sum k_{s,e}(P_i)^{(old)} \cdot q(P_i) \cdot (r_i - r)}{q(P_1) + \sum q(P_i) \cdot (r_i - r)} \quad (7)$$

In this manner points with lower quality values enhance with more probable estimates of intrinsic reflection properties, allowing to compensate the drawbacks of a time efficient calculation method.

The parameters of BRDF describing the specular lobe can be used in computer generated images of the object illuminated in an arbitrary way. However, the diffusive component, which relates to the Lambertian surface model common in colorimetry, may also be used at the stage of calculating $L^*a^*b^*$ color space as the value of L^* – simulating a perfectly ambient object illumination.

Virtual 3D Model. For use in 3D visualisation a simplified geometrical surface model is created. After geometrical data processing and triangulation described in [14], a material map with spatially varying BRDF parameters is created using adaptive texturing algorithm. Similarly as in the case of diffusive color map, a bitmap of Phong material patches is created with analogous size and texture mapping coordinates for vertices in the triangle mesh structure.

Such model can be easily imported into several 3D modelling environments and further processed. The surface can be simplified and segmented into parts of similar material properties. Finally the object can be recreated in virtual reality in real time using hardware acceleration of Phong's illumination model.

4 Exemplary Results

Procedures described above were successfully applied for processing measurement data from several test measurements. They allowed to create digital models of exemplary objects which are visible in Fig. 8. The first is a result of measurement of a figure of ancient Greek goddess Kybele, presented as a cloud of points with RGB texture. It consists of 2,8 million points. The second example is a digital model of a plaster figure of a dog, represented as a textured triangle mesh with over 40 thousand triangles.

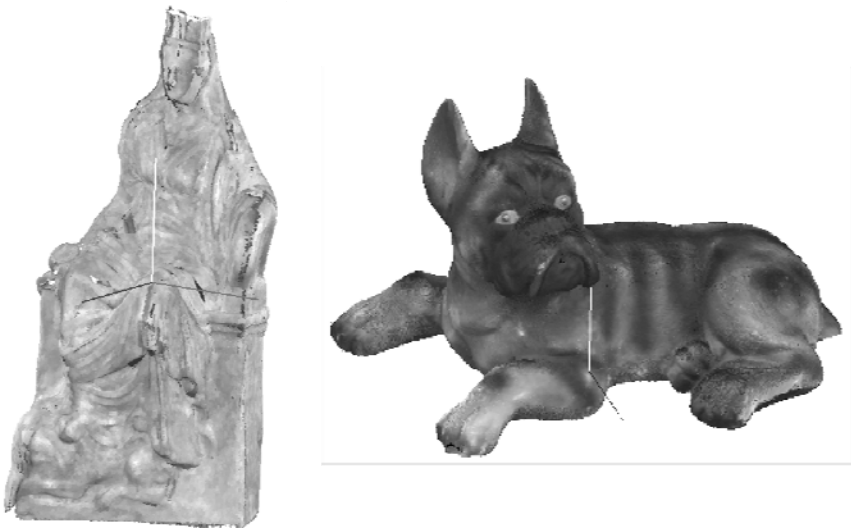


Fig. 8. Exemplary results of digital reconstruction based on the integrated measurement

Several referential measurements have been performed to determine the limitations of described processing algorithms as well as to estimate the overall error of calculated reflectance values. To verify the results, other techniques were used together with objects of well defined properties.

A spectrophotometer was used for comparison with the multispectral camera. The reflectance spectrum obtained from both devices was compared directly rather than $L^* a^* b^*$ coordinates, however both cases were investigated. GretagMakbeth Color Checker patches were used as a target for calculating spectral reflectance. The same patches were measured using the multispectral camera and their reflectance spectrum was independently estimated. After that it was possible to compare every two measured spectra and infer about quality of color measurement system. Example characteristic of the color patches measured by both devices are shown in the Fig. 9.

To verify the angular reflectance characteristics, several samples of surfaces with distinguishable reflective properties were chosen and measured independently by the

Table 1. RMS error of calculated angular reflectance characteristics compared with gonireflectometric data

Material	Class	RMS error (%)
paper	diffusive	2,8
unruffled cardboard	semi-specular	7.0
polished aluminum	shiny	1.8

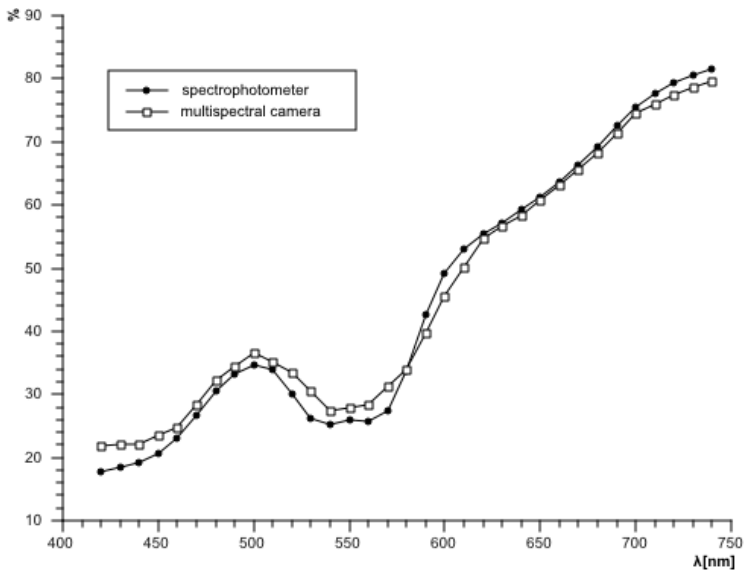


Fig. 9. Spectral characteristics comparison – filled dots resemble the measurement results from a spectrofotometer, hollow dots from a multispectral camera

measurement system and a gonireflectometric device. The objects have been grouped in classes of different BRDF profiles. Table 1 shows a collation of the estimated errors between two methods for exemplary surfaces based on RMS difference between BRDF slices. While it is still difficult to compare measurement data from different 3D measurement techniques, the overall error is less than 10% compared to reference methods, which brings a satisfactory result.

5 Summary

The paper describes data processing procedures which can be used for managing data from an integrated measurement of 3D shape, multispectral color and angular reflectance characteristic. The algorithms mentioned are divided into three stages depending on the final destination of the results. The first one serves as a digital archive and is meant to preserve as much information about object's appearance as is possible with a given measurement setup. The second stage covers procedures used for displaying purposes and allows for a creation of a digital model in a form of a triangle mesh with texture which can be exported to an independent visualisation software. The third stage produces a model which can be sent directly to a 3D printer in order to produce a faithful copy of the measured object.

The implementation of mentioned calculation methods as independent plug-ins in the 3DMADMAC calculation environment allows users to modify or exchange these procedures for custom applications.

Acknowledgements. This work was performed under the grant No. PL0097 financed by the Norwegian Financial Mechanism and EOG Financial Mechanism (2004-2009).

References

1. Pavlidis, G., Koutsoudis, A., Arnaoutoglou, F., Tsioukas, V., Chamzas, C.: Methods for 3D digitization of Cultural Heritage. *Journal of Cultural Heritage* 8(1), 93–98 (2007)
2. Imai, F.H., Rosen, M.R., Berns, R.S.: Multi-spectral imaging of Van Gogh's Self-portrait at the National Gallery of Art. In: *Proceedings of IS&T PICS Conference*, Washington, D.C, pp. 185–189. IS&T, Springfield, VA (2001)
3. Imai, F.H., Rosen, M.R., Berns, R.S.: Comparison of Spectrally Narrow-Band capture versus wide-band with a priori sample analysis for spectral reflectance estimation. In: *Proceedings of IS&T's*, pp. 234–241 (2000)
4. Conde, J., Haneishi, H., Yamaguchi, M., Ohyama, N., Baez, J.: Spectral Reflectance Estimation of Ancient Mexican Codices, Multispectral Images Approach. *Revista Mexicana de Fisica* 50, 484–489 (2004)
5. Georghiadis, A.S.: Recovering 3-D Shape and Reflectance from a Small Number of Photographs. *ACM International Conference Proceeding Series*, vol. 44, pp. 230–240 (2003)
6. Sitnik, R., Mączkowski, G., Krzesłowski, J.: Integrated Shape, Color, and Reflectivity Measurement Method for 3D Digitization of Cultural Heritage Objects. In: *Proceedings of SPIE*, vol. 7526, p. 75260Q (2010)

7. Sitnik, R.: New Method of Structure Light Measurement System Calibration Based on Adaptive and Effective Evaluation of 3D-Phase Distribution. In: Proceedings of SPIE, vol. 5856, p. 109 (2005)
8. Besl, P.J., McKay, N.D.: A Method for Registration of 3-D Shapes. *IEEE Transactions on Pattern Analysis and Machine Intelligence* 14(2), 239–256 (1992)
9. Phong, B.T.: Illumination for Computer Generated Pictures. *Communications of the ACM* 18, 311–317 (1975)
10. Sitnik, R., Kujawińska, M., Woźnicki, J.: Digital Fringe Projection System for Large-Volume 360-deg Shape Measurement. *Optical Engineering* 41, 443–449 (2002)
11. Sitnik, R., Kujawińska, M., Załuski, W.: 3DMADMAC System: Optical 3D Shape Acquisition and Processing Path for VR Applications. In: Proceedings of SPIE, vol. 5857, pp. 106–117 (2005)
12. Sitnik, R., Kujawińska, M.: From Reality to Virtual Reality: 3D Object Imaging Techniques and Algorithms. In: Proceedings of SPIE, vol. 5146, pp. 54–61 (2003)
13. Sitnik, R., Kujawińska, M.: From Cloud of Point Co-ordinates to 3D Virtual Environment: The Data Conversion System. *Optical Engineering* 41(2), 416–427 (2002)
14. Sitnik, R., Karaszewski, M.: Optimized Point Cloud Triangulation for 3D Scanning Systems. *Machine Graphics & Vision* 17, 349–371 (2008)
15. Press, W.H., Flannery, B.P., Teukolsky, S.A., Vetterling, W.T.: *Numerical Recipes in C: The Art of Scientific Computing*. Cambridge University Press, Cambridge (1992)
16. Wyszecki, G., Stiles, W.S.: *Color Science: Concepts and Methods, Quantitative Data and Formulae*. John Wiley & Sons, New York (2000)
17. Malacara, D.: *Color Vision and Colorimetry: Theory and Applications*. SPIE Press, Bellingham (2002)
18. Nicodemus, F.E., Richmond, J.C., Hsia, J.J., Ginsber, I.W., Limperis, T.: *Geometrical Considerations and Nomenclature for Reflectance*, NBS Monograph 160, U. S. Dept. of Commerce (1977)
19. Rusinkiewicz, S.: A New Change of Variables for Efficient BRDF Representation. In: Drettakis, G., Max, N. (eds.) *Rendering Techniques 1998 (Proceedings of Eurographics Rendering Workshop 1998)*, pp. 11–22. Springer, New York (1998)